Crystal Structure of an Antibody Bound to an Immunodominant Peptide Epitope: Novel Features in Peptide-Antibody Recognition

Deepak T. Nair, Kavita Singh, Naresh Sahu, Kanury V. S. Rao and Dinakar M. Salunke

J Immunol 2000;165;6949-6955

The Journal of Immunology is published twice each month by
The American Association of Immunologists, Inc.,
9650 Rockville Pike, Bethesda, MD 20814-3994.

Print ISSN: 0022-1767 Online ISSN: 1550-6606.

Crystal Structure of an Antibody Bound to an Immunodominant Peptide Epitope: Novel Features in Peptide-Antibody Recognition[1]

Deepak T. Nair,* Kavita Singh,* Naresh Sahu,† Kanury V. S. Rao,† and Dinakar M. Salunke[2]*

The crystal structure of Fab of an Ab PC283 complexed with its corresponding peptide Ag, PS1 (HQLDPAFGANSTNPD), derived from the hepatitis B virus surface Ag was determined. The PS1 stretch Gln2P to Phe7P is present in the Ag binding site of the Ab, while the next three residues of the peptide are raised above the binding groove. The residues Ser11P, Thr12P, and Asn13P then loop back onto the Ag-binding site of the Ab. The last two residues, Pro14P and Asp15P, extend outside the binding site without forming any contacts with the Ab. The PC283-PS1 complex is among the few examples where the light chain complementarity-determining regions show more interactions than the heavy chain complementarity-determining regions, and a distal framework residue is involved in Ag binding. As seen from the crystal structure, most of the contacts between peptide and Ab are through the five residues, Leu3-Asp4-Pro5-Ala6-Phe7, of PS1. The paratope is predominantly hydrophobic with aromatic residues lining the binding pocket, although a salt bridge also contributes to stabilizing the Ag-Ab interaction. The molecular surface area buried upon PS1 binding is 756 Å^2 for the peptide and 625 Å^2 for the Fab, which is higher than what has been seen to date for Ab-peptide complexes. A comparison between PC283 structure and a homology model of its germline ancestor suggests that paratope optimization for PS1 occurs by improving both charge and shape complementarity. ***The Journal of Immunology,*** **2000, 165: 6949–6955.**

Three-dimensional structures of a variety of Fab-Ag complexes have provided fine details of Ag-Fab recognition (1–3). Yet there is a lack of a unified structural model for explaining various subtle details of specificity and diversity (3). This is principally because each Ag-Ab complex is unique with respect to the binding site, although the variation in overall Ab structure is less compared with that of other proteins. Differences in the length and the nature of key residues of the complementarity-determining regions (CDRs)[3] contribute to varied topologies within the paratope (3). The wide diversity in Ag binding specificities is largely attributed to this variation in the surface features of the CDRs. The structural repertoire of CDRs does not encompass an infinite number of main chain conformations. Instead, a finite number of them appear to be used (4–6). Thus, only a limited backbone conformational repertoire in the CDRs accounts for the diversity of humoral recognition. Indeed, the nature and conformation of the amino acid side chains provide yet another level of diversity.

Among the myriad of Ags, synthetic peptides have proved to be useful model systems for the study of humoral responses. One such peptide Ag, PS1CT3, which includes a B cell epitope (segment PS1, sequence HQLDPAFGANSTNPD) derived from the large envelope protein of the hepatitis B virus and a promiscuous T cell epitope (segment CT3, sequence DIEKKIAKMEKASSVFNVVNS) (7) led to the elucidation of a variety of cellular mechanisms that guide induction and progression of T-dependent humoral responses (8, 9). A large panel of genetically distinct murine mAbs was derived from a secondary response to the peptide (7). Intriguingly, although they were derived from diverse B cell precursors, all mAbs recognized a common epitope (DPAF) within the PS1 sequence with comparable affinities (10). Thus, it can be expected that an analysis of binding of an epitope to genetically diverse Abs will provide important additional information on the nature of Ag recognition in humoral responses.

The present report details the results of our first step in this direction. We describe the crystal structure of the Fab of an IgG1κ murine mAb, PC283 (7), bound to peptide PS1. The Ab and its Fab bind to PS1 with association constants (K_a) of 2.5×10^6 and 1.02×10^6 M^{-1}, respectively, as determined using IAsys affinity biosensor (our unpublished observations). This structure provides interesting new insights concerning Ag-Ab recognition. These include preponderance of the light chain contacts with Ag, involvement of a distal framework residue in binding, and the fact that a segment of the peptide is partly raised above the binding site. Further, a comparison of the structure of mature Ab PC283 with a homology model of its germline ancestor indicates improvement of charge and shape complementarity during maturation of T-dependent humoral response against PS1.

Materials and Methods

Preparation of PC283 Fab

The Ig was precipitated from ascitic fluid with 40% ammonium sulfate. The IgG was purified from this precipitate by ion exchange chromatography using a salt gradient. The IgG was then cleaved to obtain Fab using papain (Sigma, St. Louis, MO) (11). Fab molecules were purified from the

*National Institute of Immunology and †International Center of Genetic Engineering and Biotechnology, New Delhi, India

Received for publication March 10, 2000. Accepted for publication September 20, 2000.

The costs of publication of this article were defrayed in part by the payment of page charges. This article must therefore be hereby marked *advertisement* in accordance with 18 U.S.C. Section 1734 solely to indicate this fact.

[1] This work was supported by the funds provided to the National Institute of Immunology by the Department of Biotechnology (Government of India). D.T.N. is the recipient of a fellowship from the Council of Scientific and Industrial Research (India).

[2] Address correspondence and reprint requests to Dr. Dinakar M. Salunke, Structural Biology Unit, National Institute of Immunology, Aruna Asaf Ali Marg, New Delhi 110067, India. E-mail address: dinakar@nii.res.in

[3] Abbreviations used in this paper: CDR, complementarity-determining region; rmsd, root-mean-square deviation; R_{cryst}, crystallographic R factor; R_{free}, free R factor.

0022-1767/00/$02.00

digestion mixture again by ion exchange chromatography using a salt gradient. The Fab fractions were processed to obtain a final concentration of 10 mg/ml in the crystallization buffer.

Crystallization

A number of precipitants at different concentrations were explored to crystallize the PC283 Fab-PS1 complex using the hanging drop vapor diffusion method. The crystals were obtained using a starting Fab concentration of 10 mg/ml (with a 20-fold molar excess of peptide) from the solution of 50 mM Tris-Cl, pH 7.2, after equilibrating with 18% polyethylene glycol (3.3 kDa).

Data collection

The x-ray intensity data were collected on Image Plate (Marresearch, Norderstedt, Germany) installed on a rotating anode x-ray source (RIGAKU) operated at 40 kV and 70 mA (CuKα radiation) with a nickel monochromator. The crystals diffracted up to 2.9 Å resolution and were suitable for structural studies. The crystal data and the intensity statistics are shown in Table I. It was inferred from calculations of the Matthews constant (*Vm*) (12) that there is only one Fab molecule in the asymmetric unit. The solvent content was calculated to be 43%. The intensity data were processed using DENZO (13).

Structure determination

BLAST (14) was used to search for Fab molecules in the PDB (15) that have sequence homology with PC283 for both chains. This revealed that the anti-hapten (2,2,6,6-tetramethyl 1-piperidinyloxy 2-dinitrophenyl) Fab molecule 1BAF (16) shows maximum sequence homology with PC283 (86%). Molecular replacement was conducted with 1BAF as the probe model using AMoRe (17). 1BAF gave a good correlation coefficient (32.1%) and R factor (45%), and subsequent refinement was conducted using this model.

Refinement

Further refinement was conducted using X-PLOR (18). Both conventional crystallographic R factor (R_{cryst}) and free R factor (R_{free}) (19) values (7% of total reflections) were used to monitor refinement progress. Initial rigid body refinement using whole Fab gave R_{cryst} and R_{free} of 46.8 and 46.9% respectively. On defining V_H, V_L, C_H, and C_L domains as discrete units, the rigid body refinement led to R_{cryst} and R_{free} of 33.8 and 35.1%, respectively. The model was further refined by the positional refinement protocol of X-PLOR. Electron density maps were displayed with the help of program O (20) on INDIGO (2) (Silicon Graphics, Mountain View, CA) and the sequence of 1BAF was slowly changed to that of PC283 during iterative refinement. In PC283, CDRs L1 and H3 have a single residue insertion each, and CDR L3 has a two-residue-long deletion with respect to 1BAF. However, the CDRs were not removed completely from the search model. The side chains and backbone conformations of the CDR loops were rebuilt iteratively as the density in these regions improved. After all the changes were made, and the hypervariable loops had been rebuilt, clear and empty density could be seen in the Ag binding site into which the peptide PS1 was gradually built. Initially, the stretch DPAF could be unambiguously fitted into the electron density, and the rest of the peptide could be built subsequently as the refinement progressed. Once the entire peptide model was built into the density, water molecules were added using the water-pick program in Crystallography and NMR System (21). All atoms were refined with group anisotropic B factors and were within reasonable limits. The current model has an R_{cryst} of 18.8% and an R_{free} of 26.1% using all data between 100 and 2.9 Å. The overall quality of the model was checked with PROCHECK (22). The solvent accessible area was calculated using the ACCESS-SURF module of MSI software (Molecular Simulations, San Diego, CA) based on the Lee-Richards algorithm (23) using a probe radius of 1.4 Å. The intrapeptide and Ab-peptide contacts were determined using XPLOR.

Model building

The model for the germline sequence was built using the HOMOLOGY module of the MSI software. The available germline sequence was aligned with that of the mature PC283 (Fig. 1), and the model of the germline Ab Fab was built using the coordinates of the PC283 as template. This was followed by conjugate gradient minimization of the model to remove short contacts using the DISCOVER module in which all atoms of the hypervariable loops and the side chains of the rest of the residues were allowed to move. This was followed by 50-ps molecular dynamics simulation at 300°K, in which the rest of the molecule, except for the hypervariable loops, was restrained. During the molecular dynamics simulation, conformations were written out after every 5 ps. These conformations were further subjected to conjugate gradient minimization until convergence. Distance dependent dielectric constant and consistent valence force field were used for all the energy-based computations. All energies were measured using INSIGHTII. The geometry of the least energy conformation was assessed using PROCHECK. The peptide from the PS1-PC283 crystal

Table I. *Crystal data and refinement statistics*[a]

Space group	$P2_12_12_1$
Cell constants	a = 69.298 Å, b = 72.825 Å, c = 84.783 Å
Maximum resolution	2.9 Å
Total observations	11,134
Unique reflections	7953
R_{merge} (%)	12.4 (33.3)
Completeness (%)	82 (61.1)
Multiplicity	1.4
Average (I)/(SigI)	5.1 (2.1)
No. of protein atoms3252	
No. of peptide atoms	111
No. of solvent atoms	37
R_{crys} (%)	18.8 (27.2)
R_{free} (%)	26.1 (37.5)
Refinement range (Å)	100 −2.9
rmsd bond length (Å)	0.007
rmsd bond angles (°)	1.571
Ramachandran plot	81.2% residues in core regions, 16.8% residues in allowed regions, 2% residues in generously allowed regions.
Average B value of PC283 atoms (Å^2)	24.166
Average B value of PS1 atoms (Å^2)	65.254

[a] The corresponding data for the last shell (2.90-3.03) are given in parentheses.

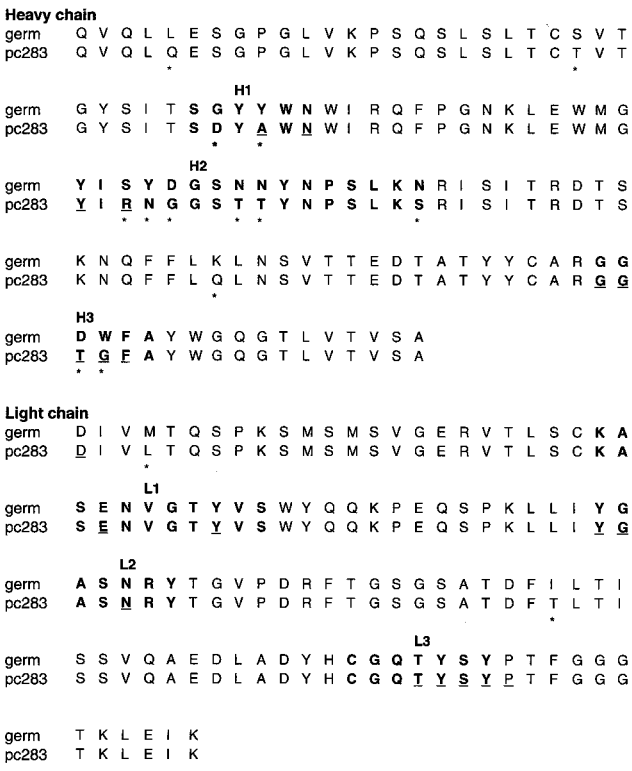

FIGURE 1. Alignment of germline and PC283 sequences. The differences are highlighted by an asterisk under the dissimilar residues. The CDRs are also highlighted in bold lettering, and their numbers are written above the sequences. The residues of PC283 which interact with the peptide are underlined.

structure was docked on the final germline model by least square superimposition of the Fv domains. The intermolecular energies between peptide and Ab were calculated using the DOCKING module of MSI software.

Results

PC283 Fab structure and the conformation of the bound PS1 peptide

The final model of the PC283-PS1 complex was built on the basis of a 2.9 Å resolution electron density map. The structure of the PC283 Fab has four standard Ig folds**,** two each for the light chain (V_L and C_L) and the heavy chain (V_H and C_H). The available sequence of PC283 was used for model building (24). Most of the PC283 Fab structure was unambiguously modeled into good electron density, although there were a few regions showing poor density. The longest stretch showing poor electron density was an exposed loop from Leu132H to Asn137H, a region that appears to be disordered in most Fab structures (25). There were also a few solvent-exposed side chains that were not observed throughout the refinement, and these residues were all modeled as alanine. During refinement, the residue Ala51L consistently showed disallowed dihedral angles. Residues at this position have been observed in other Fab structures to possess disallowed dihedral angles (26). The elbow angle of PC283 Fab was calculated to be 147°, which is within the range known to date (127–227°) for Fab molecules. It is about 10° less than that of the search model 1BAF (156°).

The 2Fo-Fc map of the peptide (Fig. 2*A*) indicated that the density for the peptide was clearly defined. The stretch Leu3P to Ala9P showed strong electron density. The terminal residues His1P and Gln2P and two of the residues propped up from the Ag combining site, Asn10P and Ser11P, showed relatively weak electron density. The stereoscopic drawing of the peptide is shown in Fig. 2*B*. The conformation of the peptide shows two consecutive β-turns formed by His1-Gln2-Leu3-Asp4 and Asp4-Pro5-Ala6-Phe7 covering the first seven residues of the peptide. The peptide shows presence of two intrapeptide hydrogen bonds between His1P and Asp4P and between Asp4P and Phe7P (Table III) corresponding to these two consecutive β-turns. The His1P side chain is raised above the binding site, so that only the backbone atoms show contacts with the hypervariable loops. The stretch Gln2P to Phe7P is present in the binding site, while the next three residues of the peptide are raised above the Ag binding groove. The residues Ser11P, Thr12P, and Asn13P then loop back onto the surface of the Ab. The last two residues, Pro14P and Asp15P, extend outside the binding site without any contacts. The looped up conformation of PS1 is evident in Fig. 3, which shows the side view of the interaction of the peptide with the Ab.

PC283 Fab-PS1 interaction

The peptide binding site is formed at the junction of light and heavy chains such that PS1 sits in a groove and is surrounded by all six CDR loops. The base and sides are formed by the residues Ala25L (L1), Val29L to Ser34L (L1), Ile47L to Gly49L (L2), and Tyr91L to Pro94L (L3) of the light chain and Ala34H (H1), Asn36H (H1), Tyr51H (H2), Arg53H (H2), and Gly99H to Phe103H (H3) of the heavy chain. The residues, which directly interact with the peptide, are shown in Fig. 4*A* (27). The CDRs H1, L2, H2, L1, H3, and L3 (in increasing order of number of interactions) together form all the 188 contacts with the peptide. The contacts constitute 181 van der Waals contacts, six hydrogen bonds, and one salt bridge (Tables II and III). CDRs L2 and H1 show very few interactions with the peptide. The light chain CDRs, L1 and L3, and the heavy chain CDR, H3, contribute most of the van der Waals contacts: 27, 75, and 50, respectively. Most of the contacts (130 of 188) are with the side chains of the peptide,

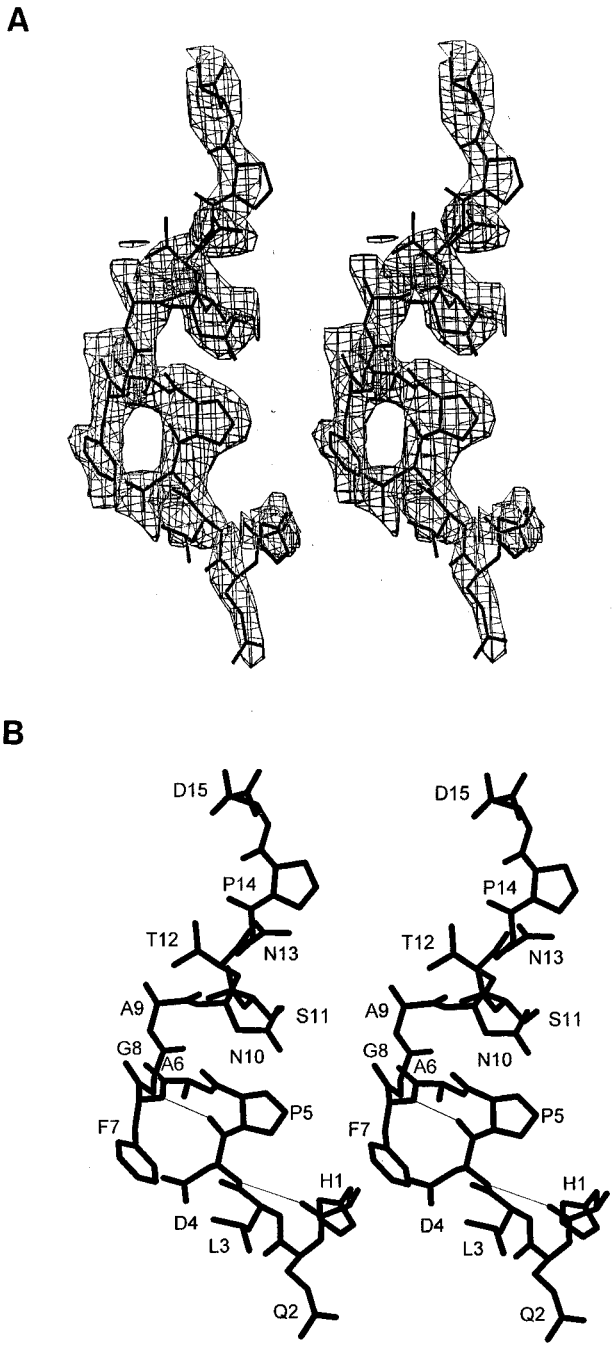

FIGURE 2. Structure of the peptide PS1. *A*, The stereoscopic drawing of the 2Fo-Fc electron density map of the peptide. The electron density is defined at the contour level of 0.8σ. *B*, The stereoscopic drawing of the PS1 peptide showing the two intrapeptide hydrogen bonds in the form of thin lines.

an observation consistent with other Ab-peptide complexes (3). Both the van der Waals contacts (Table II) and the hydrogen bonding interactions (Table III) between PS1 and PC283 are listed.

Most of the contacts of peptide with Ab are through the five residues, Leu3-Asp4-Pro5-Ala6-Phe7, of PS1. This is reflected in the average B factors of all atoms of this stretch (27 Å^2), which is much lower than the average B factors for all atoms of the entire peptide (65 Å^2). The Leu3P fits snugly into a hydrophobic groove, Asp4P forms a salt bridge with Arg53H, and Phe7P is present in a hydrophobic cup formed by the hypervariable loop residues. The

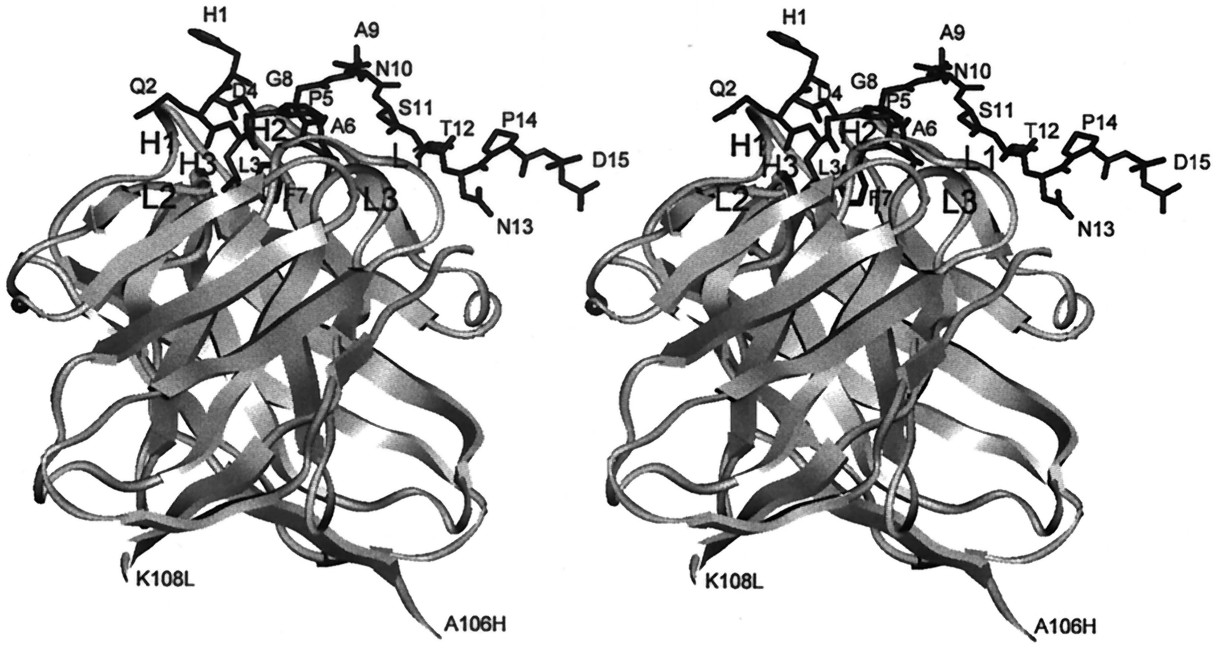

FIGURE 3. Stereoscopic model of the PC283-PS1 complex. The peptide PS1 is shown as a thick stick, and the variable domains of the PC283 Fab are shown in ribbon representation.

residues Pro5P and Ala6P also form a number of van der Waals interactions with the CDR residues. As shown in Table II, the residue stretch Ser11-Thr12-Asn13 of the peptide also forms a significant number of contacts with the Ab. While most of these contacts are with the CDR L3, the residue Asn13P also shows a significant number of interactions with the framework residue Asp1L. The side chain of the Asn13P residue is present above the residue Asp1L, as a result of which there are eight van der Waals contacts between the two residues. Only the side chain atoms of Asn13P are involved in this interaction, but in the case of Asp1L, both the side chain and the main chain atoms show contacts. Among the other residues, His1P interacts only through its main chain atoms, whereas the residues Gly8P, Ala9P, Asn10P, Pro14P, and Asp15P do not show any interactions with Ab.

The Ag binding groove is predominantly hydrophobic, with hydrophilic patches formed by Glu27L, Asn53L, and Arg53H (Fig. 4*B*). There are a number of aromatic amino acids present in the groove. The molecular surface area buried upon PS1 binding is 756 Å^2 for the peptide and 625 Å^2 for the Fab. This corresponds to about 45% of the peptide molecular surface being buried upon PS1 binding. Of the total buried molecular surface area of the Ab, 37% is from residues in the heavy chain, while the other 63% is from residues in the light chain. The percentages of accessible surface area of the framework residues, Asp1L and Ile2L, buried due to the peptide binding are 15 and 40%, respectively. For the individual peptide Ag residues, >95% of the solvent-accessible surface area of Leu3P and Phe7P is buried upon binding to PC283. Further, >75% of Asn13P is buried on binding. Thus, most of the surface area of the residues Leu3P, Phe7P, and Asn14P is buried. This is consistent with the fact that these residues collectively constitute the bulk of the contacts with Ab.

Model of the germline Ab and comparison with PC283 structure

The sequence of the germline progenitor of PC283 Ab is known (24). Compared with this, light chain of PC283 shows two changes, whereas the heavy chain shows a total of 13 changes in the sequence. The alignment of germline and PC283 sequences highlighting these changes is shown in Fig. 1. Among the interacting residues in the PS1-PC283 complex, those that have appeared through somatic mutation are Ala34H, Arg53H, Thr101H, and Gly102H in place of Tyr, Ser, Asp, and Trp, respectively.

A homology model of the germline Ab Fab was built using coordinates of PC283 as the template. The Ramchandran map showed that about 98% of the total number of residues are present in the allowed regions. The root-mean-square deviation (rmsd) between all the Cα atoms of the germline model and the Fv region of the PC283 structure was calculated to be 0.7 Å. The rmsd values for Cα atoms of all the CDR residues was 1.3 Å, with those of L3 (1.41 Å), H2 (2.1 Å), and H3 (1.3 Å) being significant. In the germline model, it is seen that the volume of the peptide binding groove is significantly lower due to the presence of Tyr in place of Ala34H, and Trp in place of Gly102H. Also, accommodation of the bulky Trp102H side chain requires the CDR H3 to move outward, away from the center of the groove. The conformations of CDRs L3 and H2 are different from those in Ab PC283 to a large extent to accommodate the bulky residue Trp102H of CDR H3 and the three mutations within H2, respectively. The remaining CDRs, L1, L2, and H1, do not show significant change in their main chain conformation. The change Ser53H to Arg is very significant, since it is observed that Arg53H in the mature Ab forms a salt bridge with Asp4P, which in terms of individual interactions provides maximum stability to the bound peptide.

Fig. 4*C* shows the surface representation of the paratope in the germline model with the peptide displayed in the same conformation as that seen in the PC283-PS1 complex. The intermolecular energy between peptide and germline Ab model was calculated to be 3×10^9 kcal/mol, which is much higher than the corresponding energy (−130 kcal/mol) between the peptide and PC283 in crystal structure. The residues Leu3P, Pro5P, Ala6P, and Phe7P show large number of short contacts with Ab residues. The residues Ser11P, Thr12P, and Asn13P also show very high number of short contacts.

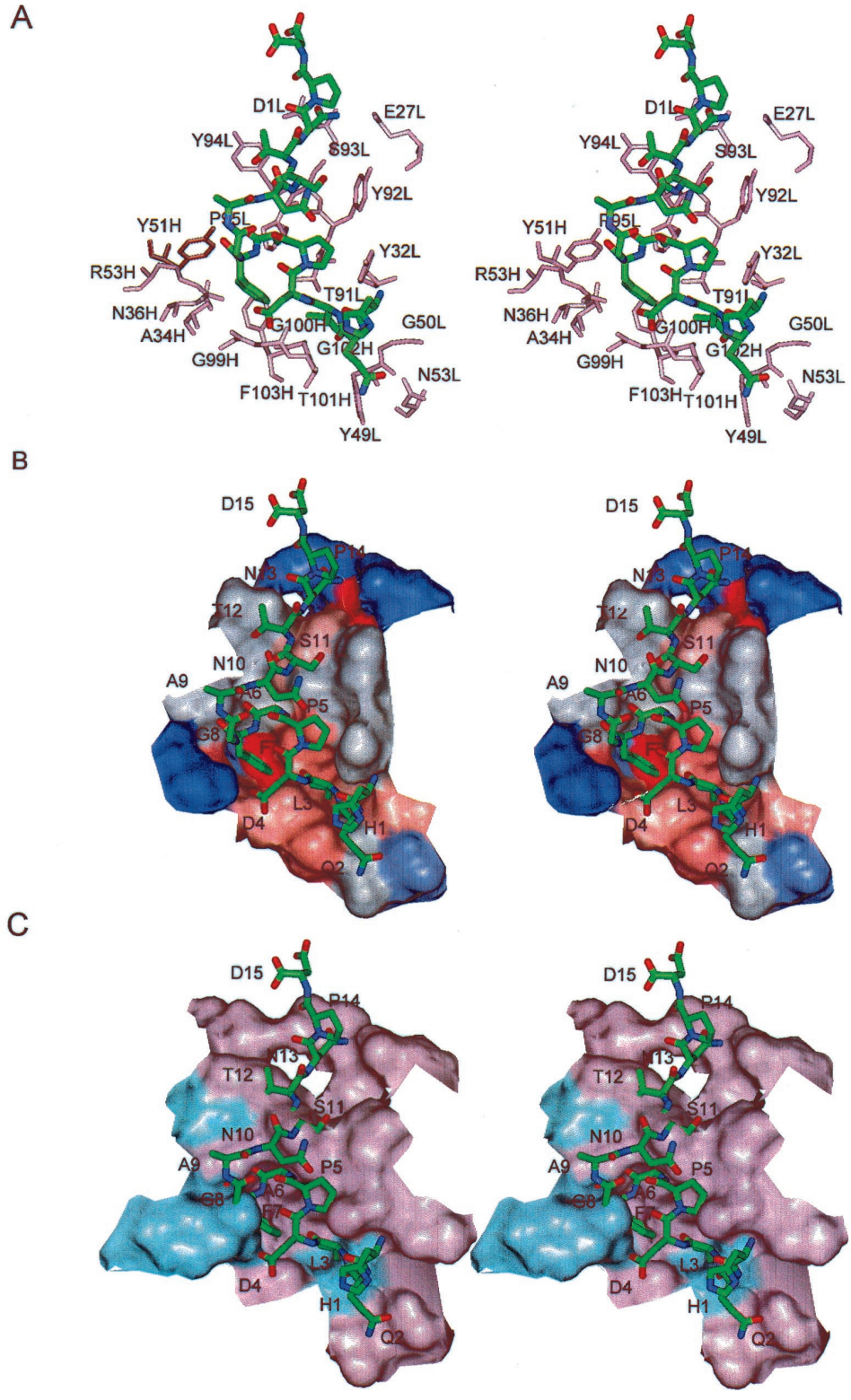

FIGURE 4. The Ag binding site of PC283. *A*, The stereoscopic drawing showing the residues of PC283 that are involved in direct contacts with the peptide PS1. The Ab residues are colored light cyan, and the peptide is shown in standard element colors. *B*, Structural features of the PC283-PS1 complex. The Connolly surface (27) of PC283 is decorated with the hydropathy feature with a color spectrum in which red to blue stands for hydrophobic to charged, respectively. The peptide residues are shown in sticks. *C*, Structural features of the germline Ab-PS1 complex. The peptide Ag (shown in sticks) is superimposed on the Connolly surface (27) of the germline PC283 model shown in light cyan. The interacting residues that are different in germline Ab compared with the matured PC283 are highlighted in light magenta.

Discussion

Peptide PS1 adopts a definite three-dimensional structure on binding to Ab PC283, with two intrapeptide hydrogen bonds contributing to two consecutive β-turns. In contrast, it has been previously observed that this peptide does not show a well-defined conformation in solution (10). The conformation of bound peptide following the β-turns is also unusual. The stretch Gly8P-Ala9P-Asn10P is raised above the binding site and forms a loop, displaying no interactions with the protein. These three residues are completely solvent accessible. The next three residues, Ser11-Thr12-Asn13, are present close to the paratope and form a large number of contacts with residues of the light chain. The presence of such centrally placed noninteracting residues in a peptide bound to an Ab is rare (25, 28).

Binding of PS1 to PC283 occurs through two nonoverlapping interaction sites. The site of primary interaction with the Ab is

Table II. *PC283-PS1 residues involved in van der Waals contacts*

Fab Residue	CDR	Peptide Residue
Heavy chain		
Ala34H	H1	Phe7P
Asn36H	H1	Phe7P
Tyr51H	H2	Phe7P; Ala6P
Arg53H	H2	Asp4P; Phe7P
Gly99H	H3	Phe7P
Gly100H	H3	Phe7P; Leu3P; Asp2P
Thr101H	H3	Gln2P; Leu3P
Gly102H	H3	Leu3P
Phe103H	H3	Phe7P
Light Chain		
Glu27L	L1	Asn13P
Tyr32L	L1	Pro5P; His1P;Leu3P
Tyr49L	L2	Gln2P; Leu3P
Gly50L	L2	Leu3P
Asn53L	L2	Gln2P
Thr91L	L3	Leu3P; Pro5P; Ala6P; Phe7P
Tyr92L	L3	Pro5P; Ser11P; Ala6P
Ser93L	L3	Ser11P; Thr12P;Asn13P; Ala6P
Tyr94L	L3	Thr12P; Asn13P
Pro95L	L3	Ala6P
Asp1L	Framework	Asn13P

Table III. *PC283-PS1 residues involved in hydrogen bonding*

Atom 1	Atom 2	Distance (Å)
Intrapeptide		
His1P: -O	Asp4P: -N	3.60
AsprP: -O	Phe7P: -N	3.50
Fab-peptide		
Tyr32L: -OH	His1P: -N	2.81
Tyr49L: -OH	Gln2P:-NE2	3.40
Thr91L: -O	Ala6P: -N	3.25
Ser93L: -OG	Ser11P: -OG	3.34
Tyr94L: -OH	Thr12P: -OG1	3.09
Arg53H: -NH2	Asp4P:-OD2	3.09
Tyr51H: -OH	Phe7P: -O	2.67

incorporated within the first seven residues of the peptide. It is evident from the crystal structure that peptide PS1 is stabilized on the paratope primarily through interactions of the stretch Leu3-Asp4-Pro5-Ala6-Phe7 with the Ab hypervariable residues. This is also consistent with the earlier findings on localizing the epitope for PC283 based on screening against overlapping PS1-derived synthetic hexapeptides (7). The residues Pro5P and Ala6P do not show as many or as strong interactions with the Ab as the other residues Leu3P, Asp4P, and Phe7P. However, they might serve to space and orient the peptide such that the side chain of Asp4P forms a salt bridge and that of Phe7P is inserted into the hydrophobic cup. Thus, a combination of van der Waals contacts and hydrogen bonds, within the peptide and with the Ab, orient and anchor the residues Leu3-Asp4-Pro5-Ala6-Phe7 of PS1 in the PC283 Ag binding site. It is appropriate to mention here that the Leu3-Asp4-Pro5-Ala6-Phe7 region of the peptide represents an immunodominant epitope recognized by PC283 as well as a series of other genetically independent mAbs raised against PS1 (7).

The residues Ser11-Thr12-Asn13 of the peptide constitute the secondary interaction site. The PC283 Fab interacts with this region primarily through the light chain CDR L3. In addition, a significant number of contacts with Asp1L, a residue belonging to the framework region, are observed. While there are other instances where framework residues have been implicated in Ag binding, these were all located proximal to the CDR residues (29, 30). The present structure must be the first case where a framework residue distal to the CDRs forms a significant number of interactions with the peptide. The involvement of such a contact in peptide recognition by germline Ab may be expected to contribute to the affinity of binding, thereby promoting selection of the corresponding B cell clonotype from the preimmune pool (31).

Table IV. *Structural features of Ab-peptide complexes*[a]

PDB Code	Ag	Solvent-Asccesible Surface Area[b] L	H	Peptide Conformation
1A3R	**VKAETRLNPDLQPTE-NH$_2$**	45.9	54.1	γ turn, type 1β turn, Asn pseudoturn, 3_{10} helix
1ACY	YNKRKRI**HIGPGRAFYT**TKNIIGC	23.6	76.4	Type II β-turn followed by type III β-turn, III-1 bend
1AI1	YNKRKRI**HIGPGR (Aib) FYT**TKNIIGC	46.1	53.9	Same as 1ACY
1BOG	**GATPEDLNQKL**AGN	41.4	58.6	Extended with 2 bends
1CE1	Ac-**TSSPSAD**	45.5	54.5	Extended
1CFN	**GATPQDLNT (norL)**	36.8	63.2	Extended with 2 bends
1CFS	**GLYEWGGARIT**NTD	48.4	51.6	Wide bend
1CFT	Efs**lkGpl**lqwrsG	48.9	51.1	Extended
1CU4	**KPKTNMKHMA**	33.6	66.4	ω turn
1F58	YNKRK**RIHIGPGR (Aib) FY**TTKNIIGC	47.2	52.8	Type I turn, followed by type VIa turn and type I turn
1FPT	CVTIMTV**DNPASTTNKDK**	29.5	70.5	S-shaped with two β-turns
1FRG	**Ac-DVPDYASL-amide**	32.8	67.2	β-turn
1GGI	**CKRIHIGPG**RAFYTTC	38.4	61.6	Turn
1HIM	**YDVPDYASL-amide**	22.4	77.6	Type 1 β-turn
1SM3	T**SAPDTRPAP**GST	31.2	68.8	Extended
1TET	VE**VPGSQHIDSQKK**A	47.4	52.6	β-turn
2F58	**JHIGPGRAFGZG**-amide	44.9	55.1	Same as 1F58
2HIP	G**LQYTPSWMLVG**	51.1	48.9	β-turn, inverse γ turn
2HRP	**MSLPGRWKPK**	50.1	49.9	β-turn
2AP2	**VVQEALDKAREGRT**	42.8	57.2	Ampipathic 3.5 turn helix
2MPA	Ac-**(Thc) KDTNNNLC*-**amide	38.3	61.7	β-turn
3F58	J**SIGPGRAFGZG**-amide	45	55	Same as IF58
2IGF	**EVVPHKK**MHKDFLEKI	20	80	type II β-turn
PC283	**HQLDPAFGANSTNPD**	62.6	37.4	Two consecutive β-turns

[a] The peptide residues for which electron density is defined are in bold and those showing interactions with the Ab are underlined.
[b] The percentage of total loss in solvent accessible surface area of Ab on peptide binding.

The PC283-PS1 complex is among the few examples where the light chain CDRs show more interactions than the heavy chain CDRs. This is contrary to the trend seen to date, with the heavy chain CDRs being more involved in forming contacts in the case of most other peptide-Ab complexes (3). The amount of the buried surface area of the peptide is much higher than the average surface area buried in similar cases (464–576 $Å^2$), observed until now (26). This is true also in case of the Ab (413–523 $Å^2$) (26). Various structural features of the PC283-PS1 complex were compared with those of other Ab-peptide complexes in the PDB (Table IV). In most cases the interacting residues of the peptide form a continuous stretch regardless of the peptide conformation. Among the few complexes that show a discontinuous epitope, PS1 has the longest stretch of noninteracting residues that are sandwiched between the primary and secondary interaction sites. The percent contributions to the total decrease in accessible surface area of the heavy and light chains on peptide binding for all the structures are listed in Table IV. It is clear that the percent contribution to the total decrease in accessible surface area of light chain in PC283-PS1 is much more than that seen for the other structures (15% more than the next highest one). Correspondingly, PC283 shows more contacts with the peptide through the light chain compared with the other anti-peptide Abs. Thus, PC283 shows an exceptionally high use of the light chain for Ag binding.

A comparison of a model of the germline progenitor with the PC283 structure could shed light on the structural basis of the changes in paratope during maturation of the PC283 Ab. Interestingly, most of the somatic mutations are in the heavy chain even though the light chain shows more contacts with the Ag in the case of mature Ab. The mutation of Ser53H to Arg leads to the formation of a salt bridge, with Asp4P enhancing the charge complementarity and thereby providing critical electrostatic stability in the Ag-Ab interaction. The binding affinity is also improved by decreasing the possibility of steric clashes, and this is achieved by mutating bulky aromatic residues (Trp102H and Tyr34H) into smaller side chains. These mutations may optimize the shape complementarity between the peptide and the Ab. Thus, it is clear that the mutations lead to an overall increase in complementarity for the immunodominant epitope Leu3-Asp4-Pro5-Ala6-Phe7. Since in the germline model the paratope appears to be dissimilar from that in the mature Ab, it is likely that the conformation of the peptide when bound to the germline Ab will be different from that seen in the crystal structure.

In summary, the structure of the PC283 complex reveals novel features adding to our understanding of Ag-Ab recognition. It is particularly intriguing that optimum somatic mutations occur primarily in the heavy chain CDRs, although the contacts with the epitope are predominantly through the light chain CDRs. Also notable is the observed involvement of a distal framework residue in establishing significant contacts with the bound Ag. Finally, our analysis indicates that the affinity maturation of PC283 occurs through optimization of critical charge interactions in addition to removal of steric clashes.

References

1. Padlan, E. A. 1996. X-ray crystallography of antibodies. *Adv. Protein Chem. 49:57.*
2. Davies, D. R., and G. H. Cohen. 1996. Interactions of protein antigens with antibodies. *Proc. Natl. Acad. Sci. USA 93:7.*
3. Wilson, I. A., and R. L. Stanfield. 1993. Antibody-antigen interactions. *Curr. Opin. Struct. Biol. 3:113.*
4. Chothia, C. and A. M. Lesk. 1987. Canonical structures for the hypervariable regions of immunoglobulins. *J. Mol. Biol. 196:901.*
5. Chothia, C., A. M. Lesk, A. Tramontano, M. Levitt, S. J. Smith-Gill, G. Air, S. Sheriff, E. A. Padlan, D. Davies, W. R. Tulip, et al. 1989. Conformations of immunoglobulin hypervariable regions. *Nature 342:877.*
6. Vargas-Madrazo, E., F. Lara-Ochoa, and J. C. Almagro. 1995. Canonical structure repertoire of the antigen binding site of immunoglobulins suggests strong geometrical restrictions associated to the mechanism of immune recognition. *J. Mol. Biol. 254:497.*
7. Agarwal, A., S. Sarkar, C. Nazabal, G. Balasundaram, and K. V. S. Rao. 1996. B cell responses to a peptide epitope. I. The cellular basis for restricted recognition. *J. Immunol. 157:2779.*
8. Nayak, B. P., A. Agarwal, P. Nakra, and K. V. S. Rao. 1999. B cell responses to a peptide epitope. VIII. Immune complex mediated regulation of memory B cell generation within germinal centers. *J. Immunol. 163:1371.*
9. Rao, K. V. S. 1999. Selection in a T-dependent primary humoral response: new insights from polypeptide models. *APMIS 107:807.*
10. Nayak, B. P., R. Tuteja, V.Manivel, R. P. Roy, R. A. Vishwakarma, and K. V. S. Rao. 1998. B cell responses to a peptide epitope. V. Kinetic regulation of repertoire discrimination and antibody optimization for epitope. *J. Immunol. 161:3510.*
11. Khurana, S., V. Rangnathan, and D. M. Salunke. 1997. The variable domain glycosylation in a monoclonal antibody specific to GnRH modulates antigen binding. *Biochem. Biophys. Res. Commun. 234:465.*
12. Matthews, B. W. 1968. Solvent content of protein crystals. *J. Mol. Biol. 33:491.*
13. Otwinowski, Z., and W. Minor. 1997. Processing of x-ray diffraction data collected in oscillation mode. *Methods Enzymol. 276:307.*
14. Madden, T. L., R. L. Tatusov, and J. Zhang. 1996. Applications of network BLAST server. *Methods Enzymol. 266:131.*
15. Bernstein, F. C., T. F. Koetzle, G. J. Williams, E. E. Meyer, Jr., M. D. Brice, J. R. Rodgers, O. Kennard, T. Shimanouchi, and M. Tasumi. 1977. The Protein Data Bank: a computer based archival file for macromolecular structures. *J. Mol. Biol. 112:535.*
16. Brunger, A. T., D. J. Leahy, T. R. Hynes, and R. O. Fox. 1991. 2.9 Å resolution structure of an anti-dinitrophenyl-spin-label monoclonal antibody Fab fragment with bound hapten. *J. Mol. Biol. 221:239.*
17. Navaza, J. 1994. AMoRe: an automated package for molecular replacement. *Acta Crystallogr. A 50:157.*
18. Brunger, A. T. 1996. *X-PLOR (Version 3.1): A System for X-ray Crystallography and NMR.* Yale University Press, New Haven.
19. Brunger, A. T. 1993. Assessment of phase accuracy by cross validation: the free R value: methods and applications. *Acta Crystallogr. D 49:24.*
20. Jones, T. A., and M. Kjeldgaard. 1994. *O–The Manual.* Uppsala University, Uppsala.
21. Brunger, A. T., P. D. Adams, G. M. Clore, W. L. Delano, P. Gros, R. W. Grosse-Kunstleve, J. S. Jiang, J. Kuszewski, M. Nilges, N. S. Pannu, et al. 1998. Crystallography and NMR system: a new software suite for macromolecular structure determination. *Acta Crystallogr. D 54:905.*
22. Laskowski, R. A., M. W. MacArthur, D. S. Moss, and J. M. Thornton. 1993. PROCHECK: a program to check the stereochemical quality of protein structures. *J. Appl. Crystallogr. 26:283.*
23. Lee, B., and F. M. Richards. 1971. The interpretation of protein structures: estimation of static accessibility. *J. Mol. Biol. 55:379.*
24. Tuteja, R. 1999. B-cell responses to a peptide epitope: mutations in heavy chain alone lead to maturation of antibody responses. *Immunology 97:1.*
25. Young, A. C. M., P. Valadon, A. Casadevall, M. D. Schraff, and J. C. Sacchettini. 1997. The three-dimensional structures of a polysaccharide binding antibody to *Cryptococcus neoformans* and its complex with a peptide from a phage display library: implications for the identification of peptide mimotopes. *J. Mol. Biol. 274:622.*
26. Dokurno, P., P. A. Bates, H. A. Band, L. M. D. Stewart, J. M. Lally, J. M. Burchell, J. Taylor-Papadimitriou, D. Snary, M. J. E. Sternberg, and P. S. Freemont. 1998. Crystal structure at 1.95 Å resolution of the breast tumor-specific antibody SM3 complexed with its peptide epitope reveals novel hypervariable loop recognition. *J. Mol. Biol. 284:713.*
27. Connolly, M. L. 1983. Solvent accessible surfaces of proteins and nucleic acids. *Science 221:709.*
28. van den Elsen, J. M. H., D. A. Kuntz, F. J. Hoedemaeker, and D. R. Rose. 1999. Antibody C219 recognizes an α-helical epitope on P-glycoprotein. *Proc. Natl. Acad. Sci. USA 96:13679.*
29. Amit, A. G., R. A. Mariuzza, S. E. V. Phillips, and R. J. Poljak. 1986. Three-dimensional structure of an antigen-antibody complex at 2.8 Å resolution. *Science 233:747.*
30. Tormo, J., D. Blaas, N. R. Parry, D. Rowlands, D. Stuart, and I. Fita. 1994. Crystal structure of a human rhinovirus neutralizing antibody complexed with a peptide derived from viral capsid protein VP2. *EMBO J. 13:2247.*
31. Rao, K. V. S. 1997. Antibody responses revisited. *Curr. Sci. 72:815.*